Protein Engineering vol.12 no.10 pp.879–884, 1999

Tryptophan H33 plays an important role in pyrimidine (6–4) pyrimidone photoproduct binding by a high-affinity antibody

Hiroyuki Kobayashi, Jiro Kato, Hiroshi Morioka, Jon D.Stewart[1] and Eiko Ohtsuka[2]

Graduate School of Pharmaceutical Sciences, Hokkaido University, Kita-ku, Sapporo 060-0812, Japan and [1]Department of Chemistry, University of Florida, Gainesville, FL 32611, USA

[2]To whom correspondence should be addressed; email: ohtsuka@pharm.hokudai.ac.jp

The importance of Trp H33 in antibody recognition of DNA containing a central pyrimidine (6–4) pyrimidone photoproduct was investigated. This residue was replaced by Tyr, Phe and Ala and the binding abilities of these mutants were determined by surface plasmon resonance and fluorescence spectroscopy. Conservative substitution of Trp H33 by Tyr or Phe resulted in moderate losses of binding affinity; however, replacement by Ala had a significantly larger impact. The fluorescence properties of DNA containing a (6–4) photoproduct were strongly affected by the identity of the H33 residue. DNA binding by both the wild-type and the W-H33-Y mutant was accompanied by a small degree of fluorescence quenching; by contrast, binding by the W-H33-F and W-H33-A mutants produced large fluorescence increases. Taken together, these variations in binding and fluorescence properties with the identity of the H33 residue are consistent with a role in photoproduct recognition by Trp H33 in the high-affinity antibody 64M5.

Keywords: antibodies/fluorescence/mutagenesis/pyrimidine (6–4) pyrimidone photoproduct/surface plasmon resonance

Introduction

Pyrimidine (6–4) pyrimidone dimers are major products of DNA photodamage that have been associated with mutation and cell death in the absence of repair (Friedberg *et al*., 1995; Sancar, 1996; Wood, 1996). *In vivo*, (6–4) photoproducts are detected and corrected efficiently by enzymes of the excision repair pathway (Jones and Wood, 1993). Because they have very high binding affinities and specificities that can be programmed by proper choice of the immunogen, monoclonal antibodies have also been explored as a means to detect and quantitate these photolesions (Roza *et al*., 1988; Mizuno *et al*., 1991; Mori *et al*., 1991; Matsunaga *et al*., 1993). While the three-dimensional structures of antibodies and repair proteins are undoubtedly quite different, it is possible that both utilize similar features to distinguish photodamage lesions in the presence of a vast excess of normal B-helical DNA. We have therefore studied a series of murine monoclonal antibodies raised against UV-irradiated calf thymus DNA (Mori *et al*., 1991). Four of these antibodies were specific for DNA containing pyrimidine (6–4) pyrimidone photoproducts in both single- and double-stranded DNA. The variable region genes for these four anti-(6–4) photoproduct antibodies have been cloned and sequenced (Morioka *et al*., 1998). Three of the four sequences (antibodies 64M2, 64M3 and 64M5) are highly related to one another; however, the 64M5 antibody binds antigen at least an order of magnitude more tightly than the 64M2 and 64M3 antibodies (Mori *et al*., 1991).

A variety of techniques have been used to examine the details of protein–DNA interactions in the series of anti-(6–4) photoproduct antibodies. Computer modeling predicted that the Fv structures of antibodies 64M2, 64M3 and 64M5 would be highly similar and that interactions with the (6–4) photoproduct itself would involve mainly non-charged interactions since the center of the combining site was predicted to possess few ionizable amino acid side chains (Morioka *et al*., 1998). On the other hand, it was observed experimentally that the affinity of the 64M5 antibody for oligonucleotides containing a central (6–4) photoproduct increased with increasing lengths up to a hexanucleotide (Kobayashi *et al*., 1998a). This suggests that electrostatic contacts might be formed between antibody side chains and phosphate groups on flanking regions of the oligonucleotides and these have been detected experimentally by ^{31}P NMR (Torizawa *et al*., 1998). A strongly cationic patch was observed on the 64M5 VH surface approximately 20 Å from the center of the combining site. Single and multiple alanine replacements for the four lysine residues making up this cationic patch were created and the properties of these mutants suggested that the region functioned in the wild-type protein as an 'electrostatic steering' element during the association phase of DNA binding, although these amino acid side chains apparently did not interact directly with the antigen after binding had occurred (Kobayashi *et al*., 1998b). Mutagenesis studies of CDR loop amino acids that differed between the 64M5 and 64M2 antibodies suggested that these proteins undergo conformational changes upon antigen binding and that the greater propensity to undergo these conformational changes is the major reason for the higher affinity of the 64M5 antibody (Kobayashi *et al*., 1999). The X-ray crystal structures of the free 64M5 Fab fragment and the 64M2 Fab fragment complexed with a d(TT) (6–4) photoproduct dimer have been solved recently (Yokoyama,H., Mizutami,R., Satow,Y., Komatsu,Y., Ohtsuka,E. and Nikaido,O., manuscript in preparation). These experimental structures were very similar to those predicted by computer modeling and comparison of the bound and free states showed the conformational changes expected from earlier studies. The apparent stacking interaction between the Trp H33 side chain and the 3′ pyrimidone nucleotide was a particularly striking feature of the 64M2 complex structure (Figure 1). This Trp residue, located in VH CDR1, is conserved in the 64M2, 64M3 and 64M5 antibodies and also in a number of other murine anti-DNA antibodies of the γ2a and γ2b subclasses (Kabat *et al*., 1992).

Stacking interactions between indole rings and nucleoside bases have been implicated in a variety of protein–DNA interactions. NMR studies have demonstrated such interactions with undamaged DNA in both model peptides (Sartorius and Schneider, 1995) and the HIV capsid protein (Morellet *et al*.,

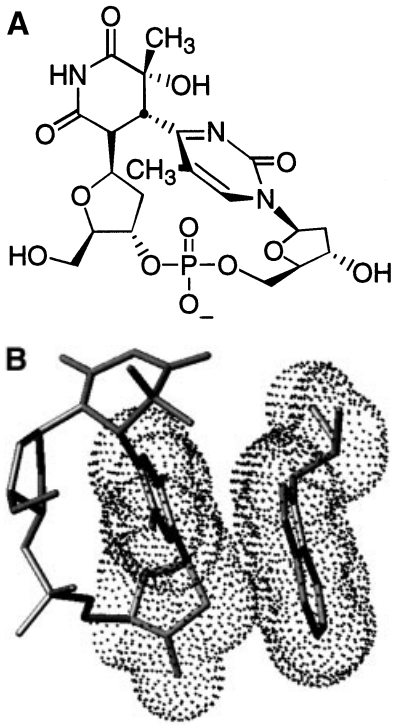

Fig. 1. Pyrimidine (6–4) pyrimidone photoproduct and its interaction with the 64M2 antibody. (**A**) Structure of the d(TT) (6–4) photoproduct. (**B**) Contact between the 64M2 Trp H33 side chain and the 3′ pyrimidone of the bound (6–4) photodimer. These coordinates were taken from the X-ray structure of this complex, which was prepared by co-crystallization with the photodimer shown in (A). Heavy atoms of both the protein and DNA are shown as heavy gray lines and the van der Waals surface of both Trp H33 and the pyrimidone portion of the photoproduct are indicated by black dots.

1998). These interactions have also been observed in damaged DNA recognition. Pi-stacking interactions between indole and methylated adenine derivatives have been investigated by small-molecule X-ray crystallography (Ishida *et al.*, 1983; Yamagata *et al.*, 1994) as models for the repair enzyme 3-methyladenine DNA glycosylase, whose crystal structure in a complex with DNA has been recently determined (Lau *et al.*, 1998). A π-stacking role for a tryptophan side chain has also been proposed for *Escherichia coli* exonuclease III (AP endonuclease VI) (Shida *et al.*, 1996).

In this paper, we examine the role of Trp H33 in photoproduct binding by the 64M5 scFv. Mutants were constructed in which this residue was substituted with phenylalanine, tyrosine or alanine. While the W-H33-F and W-H33-Y mutants retained a large fraction of the wild-type binding affinity for DNA's containing a (6–4) photoproduct, the W-H33-A substitution dramatically diminished antigen binding. Pyrimidine (6–4) pyrimidone photoproducts are fluorescent, and this property was exploited to probe the local environment of the bound antigen in the wild-type and the mutant scFvs. Taken together, our results indicate that Trp H33 plays a key role in DNA photoproduct binding by the 64M5 antibody, most likely by π-stacking interactions.

Materials and methods

General

Restriction and DNA modifying enzymes were purchased from Takara Shuzo, New England Biolabs, Bethesda Research Labs, Stratagene, Toyobo or Boehringer Mannheim. Reagents were obtained from Wako Pure Chemical Industries, Nacalai Tesque or Sigma Chemical and were used as received. DNA phosphoramidite reagents were obtained from Perkin Elmer Applied Biosystems. Routine cloning was performed according to Sambrook *et al*. (1989).

Preparation of oligonucleotides

Solid-phase oligonucleotide synthesis was carried out on an Applied Biosystems Model 394 DNA/RNA synthesizer using standard β-cyanoethyl chemistry according to the manufacturer's protocol. Oligonucleotides were purified for surface plasmon resonance measurements by reversed-phase HPLC (μBondapak C18, Waters). Those used for molecular biology techniques were purified by denaturing polyacrylamide gels. 3′-Biotinylated oligonucleotides containing a (6–4) photoproduct (T[6–4]T and CAAT[6–4]TAAG) were prepared as described previously (Kobayashi *et al.*, 1998a).

Production and isolation of mutant 64M5 scFv's

Trp H33 was replaced by alanine, phenylalanine and tyrosine using PCR methods (Higuchi, 1989) and detailed procedures have been described previously (Kobayashi *et al*., 1999). All mutant DNA sequences were confirmed by automated DNA sequencing (Applied Biosystems Model 373A). Once constructed, each mutant scFv gene was introduced into an expression plasmid in which the scFv was fused to a hexahistidine tag (Kobayashi *et al*., 1999).

All of the scFv's accumulated in *Escherichia coli* cells in the form of inclusion bodies according to SDS–PAGE and western blotting. Active proteins were obtained by solubilizing the inclusion bodies in 6 M guanidinium hydrochloride followed by an on-column refolding and purification procedure (Kobayashi *et al*., 1999). The scFv's were further purified by gel filtration using a Superose 12 HR 10/30 column equilibrated with HBS (10 mM HEPES, pH 7.4, 150 mM NaCl, 3.4 mM EDTA, 0.005% Tween-20) using a SMART-system (Pharmacia Biotech).

Surface plasmon resonance determination of (6–4) photoproduct binding by scFv's

Binding of scFv's to oligonucleotides containing a (6–4) photoproduct was measured by surface plasmon resonance (SPR) measurements using a BIAcore instrument as described previously (Kobayashi *et al*., 1999). The minimal amount of DNA was immobilized on the sensor chip in order to avoid mass transport limitations. Injections of biotinylated oligonucleotides (0.01 pmol/μl in HBS) were repeated until the SPR signal was increased by 10–30 resonance units (RU) above the original baseline. Purified scFv's were diluted in HBS buffer, then they were injected over the immobilized oligonucleotides at a flow rate of 100 μl/min over a concentration range from 10 to 200 nM. Sensorgrams were recorded and normalized to a base line of 0 RU. Equivalent volumes of diluted antibodies were also injected over a non-oligonucleotide surface to serve as blank sensorgrams to allow subtraction of the bulk refractive index background. The association was monitored by measuring the rate of binding to antigen at different protein concentrations. The dissociation of these antibodies from the antigen surface was monitored after the end of the association phase. The remaining bound antibodies were removed completely by injecting 50–100 μl 100 mM HCl. Kinetic rate constants were calculated using BIAevaluation 2.1 software (Biacore) using a single-site binding model (A + B = AB). The ratio of the

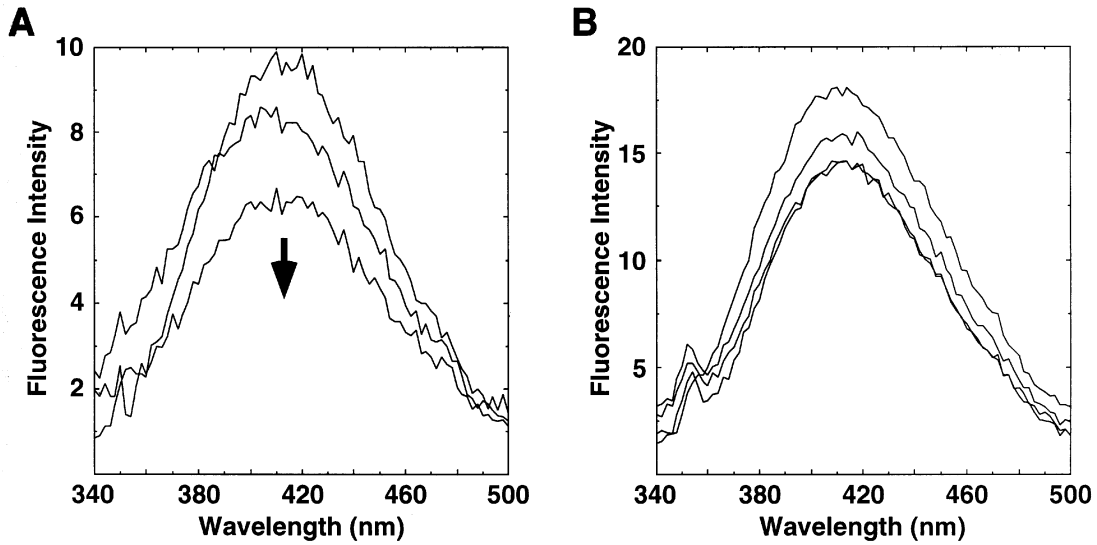

Fig. 2. Fluorescence emission spectra of the (6–4) photoproduct with excitation at 313 nm in the presence of wild-type 64M5 scFv. (**A**) Emission spectrum of 200 pmol [5′-d(CAAT(6–4)TAAG)-3′] in the presence of 0, 100 and 200 pmol wild-type 64M5 scFv. (**B**) Emission spectrum of 50 pmol [5′-d(T(6–4)T)-3′] in the presence of 0, 25, 50 and 100 pmol wild-type 64M5 scFv. No clear trend in intensity changes as a function of added scFv was observed in this case.

Table I. Kinetic constants for the binding of scFv's to oligonucleotides containing a (6–4) photoproduct

scFv	d2-mer-(6–4)[a]			d8-mer-(6–4)[b]		
	k_{ass} ($M^{-1}s^{-1}$)	k_{diss} (s^{-1})	k_{diss}/k_{ass} (M)	k_{ass} ($M^{-1}s^{-1}$)	k_{diss} (s^{-1})	k_{diss}/k_{ass} (M)
Wild type[c]	$(9.5\pm0.7)\times10^{5}$	$(1.5\pm0.2)\times10^{-3}$	$1.6\pm0.2)\times10^{-9}$	$(1.1\pm0.1)\times10^{6}$	$(1.1\pm0.2)\times10^{-4}$	$(1.0\pm0.1)\times10^{-10}$
W-H33-Y	$(9.0\pm0.1)\times10^{4}$	$(4.4\pm0.4)\times10^{-3}$	$(4.9\pm0.4)\times10^{-8}$	$(4.8\pm0.3)\times10^{5}$	$(2.1\pm0.1)\times10^{-4}$	$(4.4\pm0.3)\times10^{-10}$
W-H33-F	$(1.9\pm0.3)\times10^{4}$	$(8.4\pm0.3)\times10^{-3}$	$(4.4\pm0.7)\times10^{-7}$	$(4.5\pm0.1)\times10^{5}$	$(2.1\pm0.1)\times10^{-4}$	$(4.7\pm0.2)\times10^{-10}$
W-H33-A	ND	ND	–	$(1.3\pm0.6)\times10^{5}$	$(1.0\pm0.1)\times10^{-2}$	$(8.0\pm4.0)\times10^{-8}$

[a]d(T<6–4>T).
[b]d(CAAT<6–4>TAAG).
[c]Kobayashi *et al.* (1999).
ND, No binding detected under standard conditions.

rate constants allowed the apparent equilibrium constant to be calculated, $K_{D,app} = k_{diss}/k_{ass}$.

Fluorescence measurements of (6–4) photoproduct with scFv's

Steady-state fluorescence excitation and emission spectra of (6–4) photoproduct with scFv's were measured on a Model FP-777 spectrofluorometer (Japan Spectroscopic Co, Ltd) using a 6 mm square cuvette and a sample volume of 200 µl. The emission spectra were recorded over the wavelength range from 250 to 500 nm with an excitation wavelength of 313 nm. The spectral bandpass was 5 nm for all emission spectra. After obtaining the emission scan for the photoproduct-containing oligonucleotides alone in a HBS buffer, scFv proteins were added at the indicated concentrations and allowed to equilibrate for 30 min at 25°C prior to spectral measurements.

Results

A tryptophan at position H33 is present in all three closely-related anti-(6–4) photoproduct antibodies (64M2, 64M3 and 64M5). Moreover, the three-dimensional structures of the 64M2 and 64M5 Fab fragments determined by X-ray crystallography are highly similar (Yokoyama,H., Mizutami,R., Satow,Y., Komatsu,Y., Ohtsuka,E. and Nikaido,O., manuscript in preparation). We therefore chose to investigate the role of Trp H33 in the context of the 64M5 scFv since this antibody has the highest affinity for photoproduct-containing oligonucleotides (Mori *et al.*, 1991) and because of our previous experience in site-directed mutagenesis studies of the 64M5 scFv (Kobayashi *et al.*, 1998b, 1999). We expect the role of Trp H33 to be identical in antigen binding by the 64M2, 64M3 and 64M5 antibodies. All scFv's used in this study had the VL–linker–VH–His_6 structure that better reproduces the binding properties of the native 64M5 monoclonal antibody and the proteolytically-prepared Fab fragment (Kobayashi *et al.*, 1999).

We replaced Trp H33 by Ala, Phe and Tyr using standard site-directed mutagenesis techniques (Higuchi, 1989) and expressed the scFv proteins along with C-terminal hexahistidine tags in *E.coli* as inclusion bodies. The pure scFv proteins were prepared by solubilizing the inclusion bodies with denaturant, capturing the unfolded proteins on metal affinity columns, then re-folding the scFv proteins while still attached to the solid support (Kobayashi *et al.*, 1999). After elution from the metal affinity column, the scFv's were further purified by gel filtration chromatography. The final chromatography step also indicated that the wild-type and all three mutant scFv's were predominantly monomeric under the experimental conditions.

The rate constants for photoproduct binding by the scFv's were determined by surface plasmon resonance and the data are summarized in Table I. Two DNA's were used: the (6–4) photodimer and an octanucleotide that contained a central

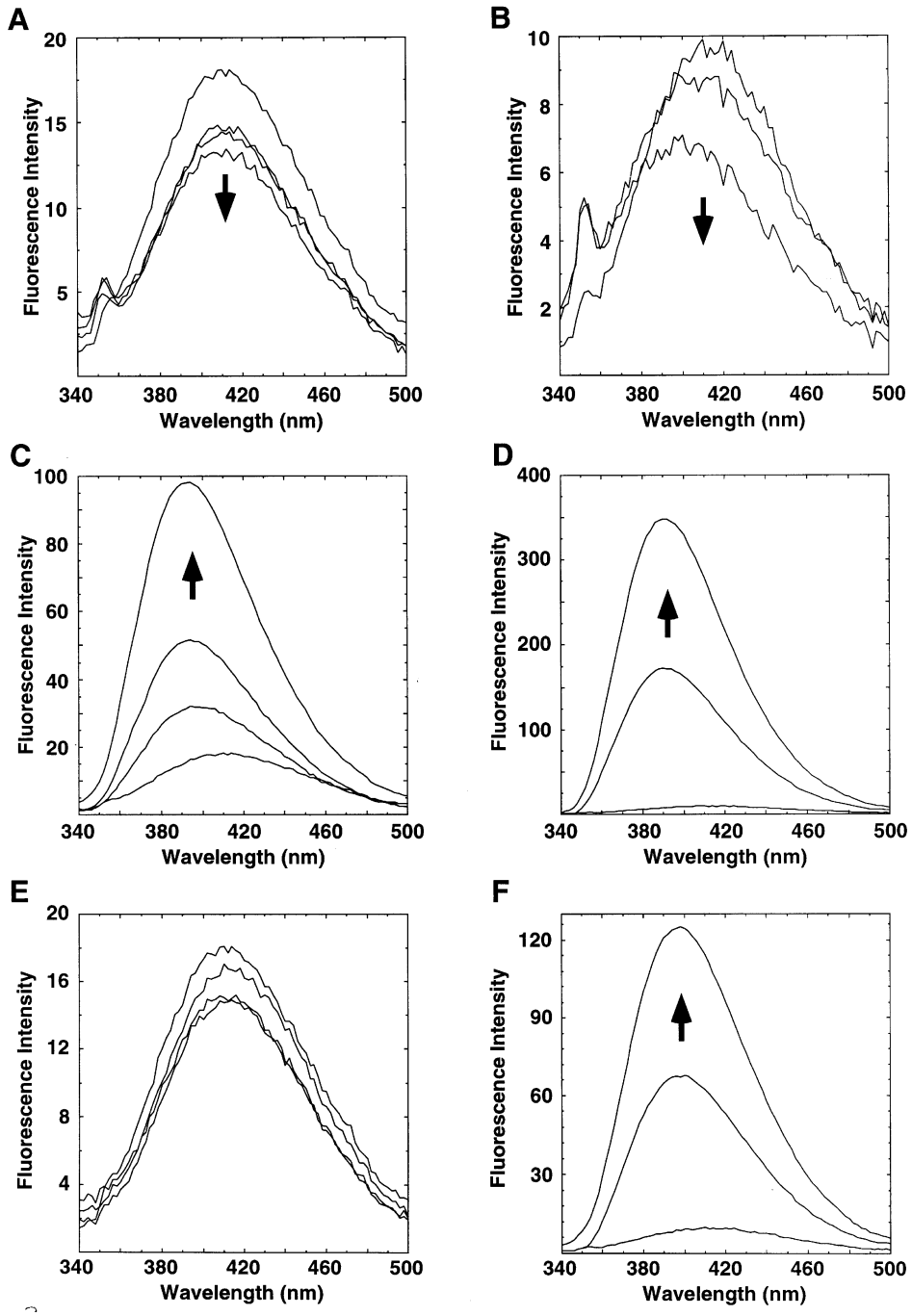

Fig. 3. Fluorescence emission spectra of the (6–4) photoproduct with excitation at 313 nm in the presence of mutant 64M5 scFv's. When observable, trends in intensity changes as a function of added scFv are indicated by arrows. (**A**) Emission spectrum of 50 pmol [5′-d(T(6–4)T)-3′] in the presence of 0, 25, 50 and 100 pmol W-H33-Y 64M5 scFv. (**B**) Emission spectrum of 200 pmol [5′-d(CAAT(6–4)TAAG)-3′] in the presence of 0, 100 and 200 pmol W-H33-Y 64M5 scFv. (**C**) Emission spectrum of 50 pmol [5′-d(T(6–4)T)-3′] in the presence of 0, 25, 50 and 100 pmol W-H33-F 64M5 scFv. (**D**) Emission spectrum of 200 pmol [5′-d(CAAT(6–4)TAAG)-3′] in the presence of 0, 100 and 200 pmol W-H33-F 64M5 scFv. (**E**) Emission spectrum of 50 pmol [5′-d(T(6–4)T)-3′] in the presence of 0, 25, 50 and 100 pmol W-H33-A 64M5 scFv. (**F**) Emission spectrum of 200 pmol [5′-d(CAAT(6–4)TAAG)-3′] in the presence of 0, 100 and 200 pmol W-H33-A 64M5 scFv.

(6–4) photoproduct. The former was designed to probe interactions with the photoproduct itself while the latter would also allow contributions to binding energy by contacts with flanking nucleotides. The W-H33-A mutant was unable to bind the dimer at detectable levels under our experimental conditions, although binding to the octamer was measurable.

The (6–4) photoproduct fluoresces with an emission maximum near 405 nm when excited at 313 nm (Hauswirth and Wang, 1977; Franklin *et al.*, 1982). Because the fluorescence properties depend on the relative torsional angle between the 5′-pyrimidine and the 3′-pyrimidone ring of the photoproduct, we exploited this technique to characterize DNA binding by the 64M5 scFv mutants. Figure 2 shows the emission spectra of the (6–4) photoproduct dimer and octamer used previously to characterize the scFv's by surface plasmon resonance. Stepwise addition of the wild-type 64M5 scFv caused a small

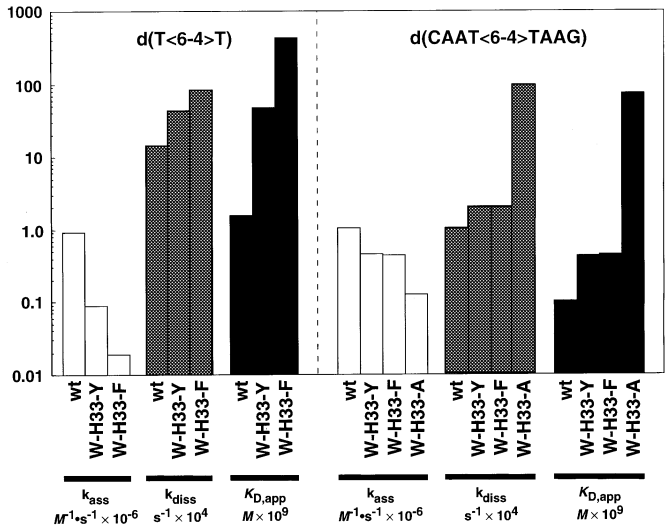

Fig. 4. Graphical representation of rate constants for photoproduct binding as determined by surface plasmon resonance.

progressive decrease in fluorescence intensity in the case of the octamer; however, only very slight changes were observed in the case of the dimer and no trend was apparent. In the case of the octamer, infinitely tight binding would be expected under the experimental conditions and the extent of fluorescence quenching as a function of added scFv was consistent with this expectation. Repeating this experiment with the W-H33-Y mutant gave similar results (Figure 3A and B). In the case of the octamer, infinitely tight binding was expected on the basis of the $K_{D,app}$ value determined by surface plasmon resonance and the data fit this expectation. In the case of the photoproduct dimer, both the DNA and the scFv concentrations were within an order of magnitude of the $K_{D,app}$ value. These data could be well described by a quadratic binding equation that incorporated the $K_{D,app}$ value determined by surface plasmon resonance (data not shown), demonstrating that both methods for detecting scFv–DNA interactions yielded consistent results and that the observed fluorescence changes are unlikely to be experimental artifacts.

When photodimer fluorescence spectra were determined in the presence of increasing concentrations of the W-H33-F mutant, large increases in fluorescence intensities were observed along with a pronounced blue shift (Figure 3C and D). Similar behavior was observed for the W-H33-A mutant (Figure 3F). These data were also consistent with quadratic binding equations incorporating $K_{D,app}$ values determined by surface plasmon resonance. Only small fluorescence changes were detected when the W-H33-A mutant was added to the (6–4) photodimer (Figure 3E), consistent with our inability to detect this interaction by surface plasmon resonance.

Discussion

While Trp commonly occurs at position H33 in anti-DNA antibodies, and it is conserved among all three closely-related anti-(6–4) photoproduct antibodies, a variety of other residues are also found in the Kabat database at this location including Ala, Phe and Tyr (Kabat *et al.*, 1992). All three H33 mutants retained the ability to bind (6–4) photoproduct-containing DNA, suggesting that the mutations did not drastically alter the native three-dimensional structure. The rate constants for (6–4) photoproduct binding by the wild-type and mutant scFv's are shown graphically in Figure 4. As would be expected for a residue that interacts strongly with the photoproduct itself, mutations of Trp H33 had the greatest impact on binding of the photodimer. The flanking nucleotides present in the octamer provide additional contacts independent of Trp H33 (Morioka *et al.*, 1998), and this reduces the impacts of all but the Ala mutation. The latter may be a special case, however, since the dramatic reduction in side chain volume may also affect the positioning of other nearby residues.

The energetic impact of removing Trp H33 on DNA binding is consistent with its proposed role in stacking with the photoproduct 3′-pyrimidone base and with the results of site-directed mutagenesis studies of Trp–DNA interactions in other proteins. For example, Voss and co-workers analyzed the consequences of mutating Trp H100A in anti-single-stranded DNA autoantibody BV04-01, whose side-chain had been shown by X-ray crystallography to stack against the central thymine base of bound d(T_3) (Rumbley *et al.*, 1993). The role and positioning of this residue is thus analogous to that of Trp H33 in our photoproduct antibodies. Substitution of Trp H100A in BV04-01 by Tyr or Phe led to decreases in K_D values of 22- and 44-fold, respectively (Rumbley *et al.*, 1993). The corresponding alterations in $K_{D,app}$ values for mutation of Trp H33 to Tyr and Phe in 64M5 are 31- and 280-fold, respectively. In the case of DNA repair protein *E.coli* photolyase, a tryptophan side chain (Trp 277) is positioned within the substrate binding pocket (Park *et al.*, 1995). While mutation of this residue to Phe or His had little effect on substrate binding, replacement by His or Arg diminished the affinity of the protein by 1000-fold (Li and Sancar, 1990).

The alterations in (6–4) photoproduct fluorescence properties with changes in the H33 residue are also consistent with a π-stacking interaction involving Trp H33. Each mutation was introduced into the X-ray crystal structure of the 64M5 scFv using computer modeling. Interestingly, the aromatic rings of both Tyr and Phe were predicted to overlap with the 3′-pyrimidone base more extensively than the indole side chain of Trp H33. While it is not possible to quantitatively interpret the fluorescence changes caused by the 64M5 scFv, we note that the decrease in (6–4) photoproduct fluorescence intensity caused by the wild type 64M5 scFv was identical to that observed for the proteolytically-prepared 64M5 Fab (data not shown), suggesting that this quenching is an intrinsic part of the binding interaction rather than an artifact of the scFv. However, we cannot determine whether these changes in fluorescence properties are due to changes in the relative angle between the pyrimidine and pyrimidone π-systems upon binding, resonance energy transfer to nearby π-systems or some other mechanism. It is clear that replacing Trp H33 with Phe or Ala alters the local environment of the (6–4) photodimer since binding is accompanied by large fluorescence increases that are not seen with the wild-type scFv.

In summary, the results of the present study argue that Trp H33 plays a key role in (6–4) photoproduct binding by the high-affinity 64M5 antibody. Whether enzymes that recognize and repair these photolesions will also utilize a similar interaction with the 3′-pyrimidone base remains to be determined.

Acknowledgements

We thank Dr Yoshinori Satow (University of Tokyo) for permission to use the coordinates of the crystal structures cited in this work and Drs Yasuo Komatsu (Hokkaido University), Koichi Kato (University of Tokyo) and Ichio Shimada (University of Tokyo) for valuable discussions. This work was

supported by Grants-in-Aid by the Monbusho International Scientific Research Program and by Specially Promoted Research funding from the Ministry of Education, Science, Culture and Sports of Japan.

References

Franklin,W.A., Lo,K.M. and Haseltine,W.A. (1982) *J. Biol. Chem.*, **257**, 13535–13543.

Friedberg,E.C., Walker,G.C. and Siede,W. (1995) In *DNA Repair and Mutagenesis*. ASM Press, Washington, DC.

Hauswirth,W., and Wang,S.Y. (1977) *Photochem. Photobiol.*, **25**, 161–166.

Higuchi,R. (1989) In Erlich,H.A. (ed.), *PCR Technology*. Stockton Press, New York, pp. 61–70.

Ishida,T., Shibata,M., Fujii,K. and Inoue,M. (1983) *Biochemistry*, **22**, 3571–3581.

Jones,C.J. and Wood,R.D. (1993) *Biochemistry*, **32**, 12096–12104.

Kabat,E.A., Wu,T.T., Perry,H.M., Gottesman,K.S. and Foeller,C. (1992) *Sequences of Proteins of Immunological Interest*, Release 5.0. National Institutes of Health, Bethesda, MD. The most up-to-date release can be found at http://www.immuno.bme.nwu.edu

Kobayashi,H., Morioka,H., Torizawa,T., Kato,K., Shimada,I., Nikaido,O. and Ohtsuka,E. (1998a) *J. Biochem.*, **123**, 182–188.

Kobayashi,H., Morioka,H., Nikaido,O., Stewart,J.D. and Ohtsuka,E. (1998b) *Protein Engng*, **11**, 1089–1092.

Kobayashi,H., Morioka,H., Tobisawa,K., Torizawa,T., Kato,K., Shimada,I., Nikaido,O., Stewart,J.D. and Ohtsuka,E. (1999) *Biochemistry*, **38**, 532–539.

Lau,A.Y., Scharer,O.D., Samson,L., Verdine,G.L. and Ellenberger,E. (1998) *Cell*, **95**, 249–258.

Li,Y.F. and Sancar,A. (1990) *Biochemistry*, **29**, 5698–5706.

Matsunaga,T., Hatakeyama,Y., Ohta,M., Mori,T. and Nikaido,O. (1993) *Photochem. Photobiol.*, **57**, 934–940.

Mizuno,T., Matsunaga,T., Ihara,M. and Nikaido,O. (1991) *Mutat. Res.*, **254**, 175–184.

Morellet,N., Demene,H., Teilleux,V., Huynh-Dinh,T., de Rocquigny,H., Fournie-Zaluski,M.C. and Roques,B.P. (1998) *J. Mol. Biol.*, **283**, 419–434.

Mori,T., Nakane,M., Hattori,T., Matsunaga,M., Ihara,M. and Nikaido,O. (1991) *Photochem. Photobiol.*, **54**, 225–232.

Morioka,H., Miura,H., Kobayashi,H., Koizumi,T., Fujii,K., Asano,K., Matsunaga,T., Nikaido,O., Stewart,J.D. and Ohtsuka,E. (1998) *Biochim. Biophys. Acta*, **1385**, 17–32.

Park,H.-W., Kim,S.-T., Sancar,A. and Deisenhofer,J. (1995) *Science*, **268**, 1866–1872.

Roza,L., Van der Wulp,K.J.M., Macfarlane,S.J., Lohman,P.H.M. and Baan,R.A. (1988) *Photochem. Photobiol.*, **48**, 627–633.

Rumbley,C.A., Denzin,L.K., Yanta,L., Tetin,S.Y. and Voss,E.W.,Jr (1993) *J. Biol. Chem.*, **268**, 13667–13674.

Sambrook,J., Fritsch,E.F. and Maniatis,T. (1989) *Molecular Cloning: A Laboratory Manual*, 2nd Edn. Cold Spring Harbor Laboratory Press, Cold Spring Harbor.

Sancar,A. (1996) *Annu. Rev. Biochem.*, **65**, 43–81.

Sartorius,J. and Schneider,H.J. (1995) *FEBS Lett.*, **374**, 387–392.

Shida,T., Noda,M. and Sekiguchi,J. (1996) *Nucleic Acids Res.*, **24**, 4572–4576.

Torizawa,T., Kato,K., Kimura,Y., Asada,T., Kobayashi,H., Komatsu,Y., Morioka,H., Nikaido,O., Ohtsuka,E. and Shimada,I. (1998) *FEBS Lett.*, **429**, 157–161.

Wood,R.D. (1996) *Annu. Rev. Biochem.*, **65**, 135–167.

Yamagata,Y., Kato,M. and Fujii,S. (1994) *Chem. Pharm. Bull.*, **42**, 2385–2387.

Received February 26, 1999; revised May 24, 1999; accepted June 21, 1999